

## Resonance Raman Spectroscopic Studies on the Group 6B Polyatomic Cations $S_4^{2+}$ , $Se_4^{2+}$ , and $Te_4^{2+}$ †

Robin J. H. Clark,\* Trevor J. Dines, and Lindsay T. H. Ferris

Christopher Ingold Laboratories, University College London, 20 Gordon Street, London WC1H 0AJ

The Raman and resonance Raman (r.R.) spectra of  $S_4^{2+}$  and  $Se_4^{2+}$  in oleum at room temperature, of  $Te_4^{2+}$  in  $H_2SO_4$ , and of  $Te_4[Al_2Cl_7]_2$  at ca. 80 K, have been recorded with a variety of excitation lines. The r.R. spectra display long progressions,  $\nu_1\nu_1$ , in the  $\nu_1$  ( $a_{1g}$ ) mode in each case, together with shorter progressions of the sort  $\nu_1\nu_1 + \nu_2$  ( $b_{1g}$ ). Analysis of the results leads to harmonic wavenumbers ( $\omega_1$ ) of 584.7, 321.8, and 219.5  $cm^{-1}$  for  $S_4^{2+}$ ,  $Se_4^{2+}$ , and  $Te_4^{2+}$ , respectively, in solution, and anharmonicity constants ( $x_{11}$ ) of  $-0.35$ ,  $-0.55$ , and  $-0.30$   $cm^{-1}$ , respectively. Stretching force constants (valence force field) for  $S_4^{2+}$ ,  $Se_4^{2+}$ , and  $Te_4^{2+}$  in solution are calculated to be 2.78, 2.10, and 1.45  $mdyn \text{ \AA}^{-1}$ , respectively, the *trans*-bond stretch-stretch interaction constants being more than an order of magnitude greater than the *cis*-bond ones. The  $\nu_1$  band excitation profile of each ion maximises within the band contour of the lowest allowed electronic transition of each ion, i.e. that at 330 nm for  $S_4^{2+}$ , 410 nm for  $Se_4^{2+}$ , and 510 nm for  $Te_4^{2+}$ . These data, coupled with detailed measurements on the Raman band polarizations at resonance, indicate that the assignment of the lowest allowed transition of each ion is  $\pi^*(b_{2u}) \leftarrow \pi(e_g)$ ,  ${}^1E_u \leftarrow {}^1A_{1g}$ .

The chemistry of sulphur, selenium, and tellurium in highly acidic media has been studied extensively,<sup>1-5</sup> and it has been shown that these elements are oxidized to form intensely coloured polyatomic cationic species. Using a combination of physicochemical techniques, involving cryoscopic, conductometric, and spectroscopic measurements, Gillespie and co-workers<sup>5-15</sup> have established the presence of  $S_{19}^{2+}$ ,  $S_8^{2+}$ ,  $S_4^{2+}$ ,  $Se_{10}^{2+}$ ,  $Se_8^{2+}$ ,  $Se_4^{2+}$ ,  $Te_6^{4+}$ , and  $Te_4^{2+}$  in acidic solutions. X-Ray crystallographic measurements on  $Se_4[HS_2O_7]_2$ , and on compounds obtained from melts containing M,  $MCl_4$ , and  $AlCl_3$  (M = Se or Te), have established a square-planar ( $D_{4h}$ ) geometry for the  $M_4^{2+}$  species<sup>10,16,17</sup> and a bicyclic structure for  $Se_8^{2+}$ .<sup>8</sup> The square-planar geometry for the  $M_4^{2+}$  ions gives rise to the following molecular vibrations:  $\nu_1$  ( $a_{1g}$ ),  $\nu_2$  ( $b_{2g}$ ), and  $\nu_3$  ( $b_{1g}$ ) (all Raman active),  $\nu_4$  ( $b_{2u}$ ) (inactive), and  $\nu_5$  ( $e_u$ ) (i.r. active);  $\nu_4$  is an out-of-plane motion, but the other modes are all in-plane. I.r. and Raman spectroscopic measurements have confirmed the  $D_{4h}$  structure for the ions in solution although a lowering of symmetry, resulting in site- and factor-group effects, has been deduced from solid-state spectra.

Molecular orbital calculations on the  $M_4^{2+}$  species have been carried out;<sup>15,18-21</sup> the  $\pi$ -orbital levels are shown in Figure 1. The ions are examples of  $6\pi$ -electron systems, and they are thus examples of inorganic aromatic compounds. Their  $\pi$ -bond order is 0.25 (0.50 according to the Hückel molecular-orbital definition of  $\pi$ -electron bond order, this strictly relating to the electron occupancy number of the  $\pi$  orbitals<sup>20</sup>), and so the overall M-M (valence bond) bond order is 1.25. The ions can be regarded as examples of 'class III' mixed-valence species, owing to the equivalence of each atom both structurally and with respect to charge (+0.5). The lowest allowed electronic transition for these ions assuming  $D_{4h}$  symmetry is  $\pi^* \leftarrow \pi$  ( ${}^1E_u \leftarrow {}^1A_{1g}$ ), i.e. that corresponding to the transition of an electron from the non-bonding  $e_g$  orbital to the antibonding  $b_{2u}$  orbital. These transitions are thought to give rise to the bands at 330, 410, and 510 nm for  $S_4^{2+}$ ,  $Se_4^{2+}$ , and  $Te_4^{2+}$ , respectively. Booth *et al.*<sup>22</sup> have obtained resonance Raman (r.R.) spectra on the  $Te_4^{2+}$  ion in  $H_2SO_4$  solution by excitation with the 514.5 nm line of an argon-ion laser, the most prominent

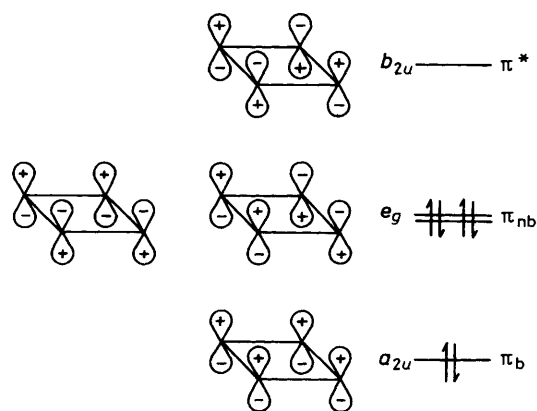


Figure 1.  $\pi$  Molecular orbital scheme for the  $M_4^{2+}$  species; b = bonding, nb = non-bonding

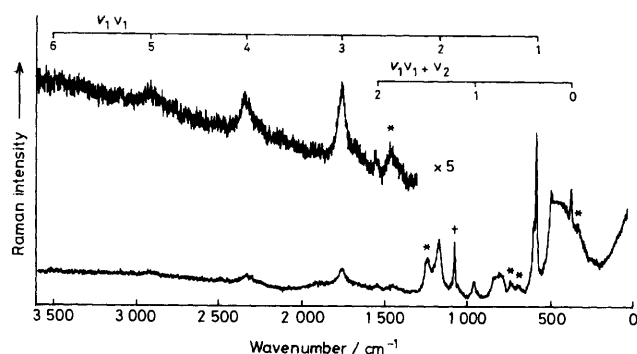
feature being an overtone progression  $\nu_1\nu_1$ , extending to  $\nu_1 = 4$ . No r.R. studies of  $Se_4^{2+}$  and  $S_4^{2+}$  have yet been reported, presumably because their lowest energy absorption bands lie to shorter wavelengths than those of laser lines commonly available. However, by the use of violet and u.v. exciting lines from a high power krypton-ion laser, we have successfully measured the r.R. spectra of  $Se_4^{2+}$  and  $S_4^{2+}$ . These results are reported in the present study, together with some improved r.R. data on the  $Te_4^{2+}$  ion. Raman band polarization data lead to confirmation of the assignment of the resonant transitions.

### Experimental

(a) *Sample Preparation.*— $Te_4^{2+}$  was generated by dissolving elemental tellurium in concentrated  $H_2SO_4$ , and studied within 24 h owing to the slow precipitation of  $TeO_2$ .  $Te_4[Al_2Cl_7]_2$  was prepared by heating elemental tellurium with  $TeCl_4$  and  $AlCl_3$  in an evacuated sealed tube at 260 °C for ca. 1 week.<sup>16</sup>  $Se_4^{2+}$  was generated by dissolving elemental selenium in 25% oleum to produce  $Se_8^{2+}$ , which was then oxidized to  $Se_4^{2+}$  with  $[NH_4]_2[S_2O_8]$ .<sup>4</sup>  $S_4^{2+}$  was prepared by dissolving elemental sulphur in 65% oleum.<sup>3</sup> This solution contains  $S_4^{2+}$ ,  $S_8^{2+}$ , and  $S_{16}^{2+}$ ; it is deep blue due to the 590

† Presented in part at the N.A.T.O. Advanced Study Institute on Mixed-valence compounds, Oxford, 1979.

Non-S.I. unit employed: 1 dyn =  $10^{-5}$  N.



**Figure 2.** Resonance Raman spectrum of a solution of  $S_4^{2+}$  in 65% oleum recorded with 350.7 nm excitation. Power at the sample = 100 mW, scan speed =  $1 \text{ cm}^{-1} \text{ s}^{-1}$ , time constant = 1 s, and spectral slitwidth =  $5 \text{ cm}^{-1}$  at 350.7 nm. The bands marked (\*) are due to oleum, the one at  $1071 \text{ cm}^{-1}$  marked (†) is due to  $SO_3$  present in the oleum, and the broad features centred on ca.  $450 \text{ cm}^{-1}$  and ca.  $800 \text{ cm}^{-1}$  are due to Raman scattering from the silica cell

**Table 1.** Details of the r.R. spectrum <sup>a</sup> of  $S_4^{2+}$  in 65% oleum

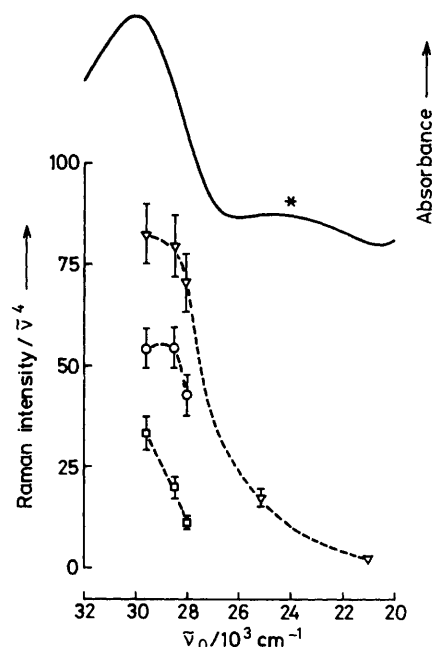
Assignment	$\tilde{\nu}/\text{cm}^{-1}$	f.w.h.m./ $\text{cm}^{-1}$	Relative intensity	$\rho(\pi/2)$
$\nu_2 (b_{1g})$	$371.2 \pm 0.5$	$12 \pm 1$	0.30	$0.65^b$
$\nu_1 (a_{1g})$	$583.6 \pm 0.5$		1.00	$0.17^c$
$\nu_3 (b_{2g})$	$598.1 \pm 0.5$		0.37	$0.50^b$
$\nu_1 + \nu_2 (B_{2g})$	$953.7 \pm 0.5$		0.15	
$2\nu_1 (A_{1g})^d$	$1168.1 \pm 0.5$	$32 \pm 2$	0.68	
$2\nu_1 + \nu_2 (B_{1g})$	$1539 \pm 2$		0.05	
$3\nu_1 (A_{1g})$	$1750 \pm 2$	$45 \pm 5$	0.24	
$4\nu_1 (A_{1g})$	$2332 \pm 5$		0.19	
$5\nu_1 (A_{1g})$	$2912 \pm 5$		0.11	
$6\nu_1 (A_{1g})$	$3480 \pm 10$		0.05	

<sup>a</sup>  $\lambda_0 = 350.7 \text{ nm}$ . <sup>b</sup>  $\pm 0.05$ . <sup>c</sup>  $\pm 0.02$ . <sup>d</sup> Possibly overlapped by  $\nu_1 + \nu_3$ .

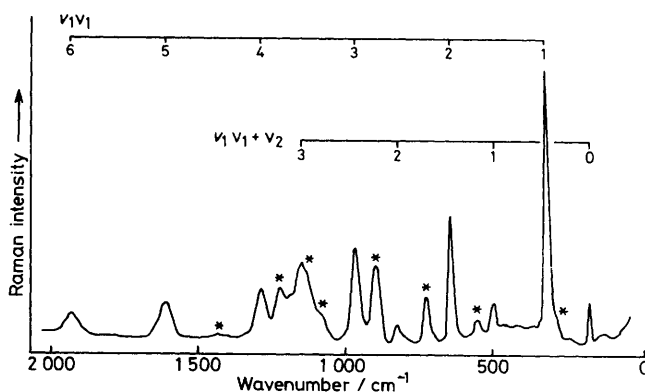
nm absorption band of the  $S_8^{2+}$  species. For Raman measurements the solutions were sealed in either Pyrex or silica cells, which were spun at  $>1000 \text{ r.p.m.}$  to minimize thermal and photochemical decomposition. The spectra of solid  $Te_4[Al_2Cl_7]_2$  were recorded at 80 K using a cell cooled with liquid nitrogen.

(b) *Raman Spectroscopy.*—Raman spectra were recorded using Spex 1401 and 14018 (Ramalog 6) spectrometers in conjunction with Coherent Radiation model CR15UV argon-ion and CR3000K krypton-ion lasers, and a Coherent Radiation model CR490 dye laser employing stilbene-3 as the lasing medium (some of the measurements on  $Se_4^{2+}$  were obtained using a Jobin-Yvon Ramanor spectrometer with a Spectra Physics 170 krypton-ion laser, by courtesy of Dr. R. E. Hester, University of York). Band wavenumber measurements were calibrated using the emission spectrum of neon, and band intensities, determined as the product of peak height and full width at half-maximum (f.w.h.m.) were corrected for the spectral response of the appropriate spectrometer. Measurements of depolarization ratios in the u.v. region were obtained using a Polaroid HNP'B linear polarizer. Resolution of overlapping bands was performed using a Nicolet 1180 computer interfaced to the Spex Ramalog 6 spectrometer.

(c) *Electronic Absorption Spectroscopy.*—Electronic absorption spectra were obtained from solutions in silica cuvettes using a Cary 14 spectrophotometer.



**Figure 3.** Excitation profiles of the  $\nu_1$  ( $\nabla$ ),  $2\nu_1$  ( $\circ$ ), and  $3\nu_1$  ( $\square$ ) bands of  $S_4^{2+}$ , together with the absorption spectrum of the ion. The band marked (\*) in the absorption spectrum is due to the  $S_{16}^{2+}$  species which is also present in the solution



**Figure 4.** Resonance Raman spectrum of a solution of  $Se_4^{2+}$  in 25% oleum recorded with 406.7 nm excitation. Power at the sample = 100 mW, scan speed =  $1 \text{ cm}^{-1} \text{ s}^{-1}$ , time constant = 1 s, and spectral slitwidth =  $5 \text{ cm}^{-1}$  at 406.7 nm. The bands marked (\*) are due to oleum

## Results

(a)  $S_4^{2+}$ .—The Raman spectrum of a solution of sulphur in 65% oleum was recorded for laser excitation in the range 337.5–476.2 nm. Excitation at longer wavelengths results in strong luminescence, believed to be due to the presence of the  $S_8^{2+}$  species ( $\lambda_{\text{max.}} = 590 \text{ nm}$ ). No Raman bands attributable to either  $S_8^{2+}$  or  $S_{16}^{2+}$  were observed with any exciting lines, probably because these species are present in lower concentrations than is  $S_4^{2+}$ , and decrease in concentration with time. However, it was found that excitation with u.v. laser lines caused a regeneration of  $S_8^{2+}$ , as evidenced by a deepening of the blue colour of the solution, most markedly at the laser focus.

Excitation with lines which fall within the contour of the 330 nm band ( $\epsilon_{\text{max.}} = 2200 \text{ dm}^3 \text{ mol}^{-1} \text{ cm}^{-1}$ )<sup>9</sup> produced r.R.

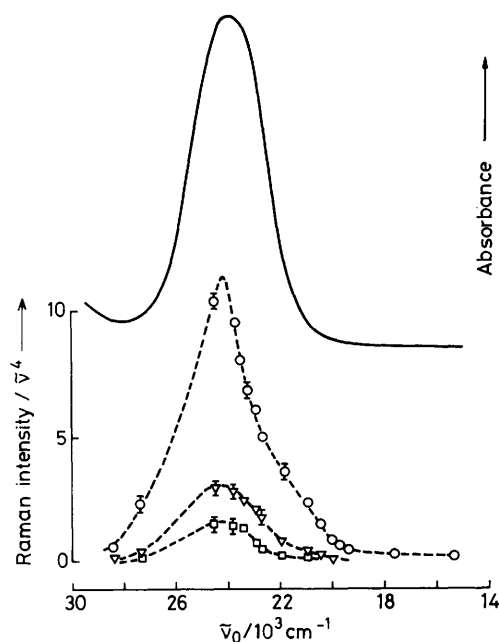


Figure 5. Excitation profiles of the  $\nu_1$  (○),  $2\nu_1$  (▽), and  $3\nu_1$  (□) bands of  $\text{Se}_4^{2+}$ , together with the absorption spectrum of the ion

Table 2. Details of the r.R. spectrum <sup>a</sup> of  $\text{Se}_4^{2+}$  in 25% oleum

Assignment	$\tilde{\nu}/\text{cm}^{-1}$	f.w.h.m./ $\text{cm}^{-1}$	$\rho(\pi/2)$
$\nu_2 (b_{1g})$	$182.3 \pm 0.5$	16	0.70
$\nu_1 (a_{1g})$	$321.3 \pm 0.5$	10	0.33
$\nu_3 (b_{2g})$			
$\nu_1 + \nu_2 (B_{1g})$	$501 \pm 1$	25	0.36
$2\nu_1 (A_{1g})$ <sup>b</sup>	$639.6 \pm 0.5$	15	
$2\nu_1 + \nu_2 (B_{1g})$	$819 \pm 1$	32	
$3\nu_1 (A_{1g})$	$957.4 \pm 0.5$	24	
$3\nu_1 + \nu_2 (B_{1g})$	$1\ 136 \pm 2$		
$4\nu_1 (A_{1g})$	$1\ 275 \pm 1$	40	
$5\nu_1 (A_{1g})$	$1\ 592 \pm 1$	48	
$6\nu_1 (A_{1g})$	$1\ 910 \pm 2$	60	

<sup>a</sup>  $\lambda_0 = 406.7$  nm. <sup>b</sup> Possibly overlapped by  $\nu_1 + \nu_3$ .

spectra of  $\text{S}_4^{2+}$  (colourless), characterized by an overtone progression in  $\nu_1\nu_1$ , extending to  $\nu_1 = 6$ , and a combination band progression  $\nu_1\nu_1 + \nu_2$ , extending to  $\nu_1 = 2$ . The third Raman-active fundamental,  $\nu_3 (b_{2g})$ , is observed as a shoulder on the high-wavenumber side of  $\nu_1$ , and it is possible that a progression of the type  $\nu_1\nu_1 + \nu_3$  overlaps that of  $\nu_1\nu_1$ . The r.R. spectrum of  $\text{S}_4^{2+}$  is shown in Figure 2 and the band wavenumber measurements, assignments, depolarization ratios, and bandwidths (f.w.h.m.) are given in Table 1. The assignments of the  $\text{S}_4^{2+}$  bands were confirmed by recording r.R. spectra of solutions containing different concentrations of  $\text{S}_4^{2+}$ . Although the concentration of  $\text{S}_4^{2+}$  in the solutions decreases with time, we were able to obtain approximate excitation profiles for  $\nu_1$ ,  $2\nu_1$ , and  $3\nu_1$  using the  $1\ 071$   $\text{cm}^{-1}$  band of the  $\text{SO}_3$  present in the oleum as internal standard. These profiles are shown, together with the absorption spectrum, in Figure 3.

(b)  $\text{Se}_4^{2+}$ .—The lowest allowed electronic band of  $\text{Se}_4^{2+}$  (yellow-orange) maximizes at 410 nm, with  $\epsilon_{\text{max.}} = 8\ 000$   $\text{dm}^3 \text{mol}^{-1} \text{cm}^{-1}$ .<sup>7</sup> The r.R. spectrum of  $\text{Se}_4^{2+}$  in 25% oleum, obtained with 406.7 nm excitation, is shown in Figure 4; it is

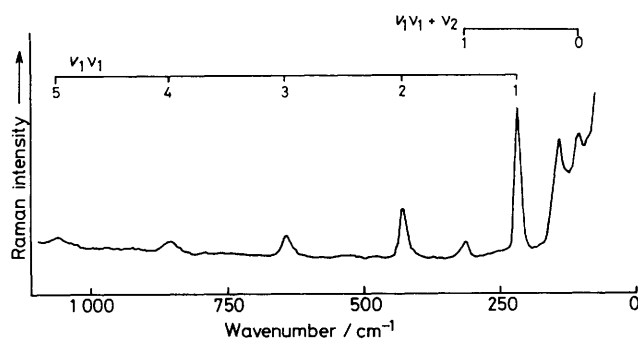


Figure 6. Resonance Raman spectrum of  $\text{Te}_4[\text{Al}_2\text{Cl}_7]_2$  at 80 K recorded with 514.5 nm excitation. Power at the sample = 100 mW, scan speed =  $1 \text{ cm}^{-1} \text{ s}^{-1}$ , time constant = 1 s, and spectral slitwidth =  $5 \text{ cm}^{-1}$  at 514.5 nm

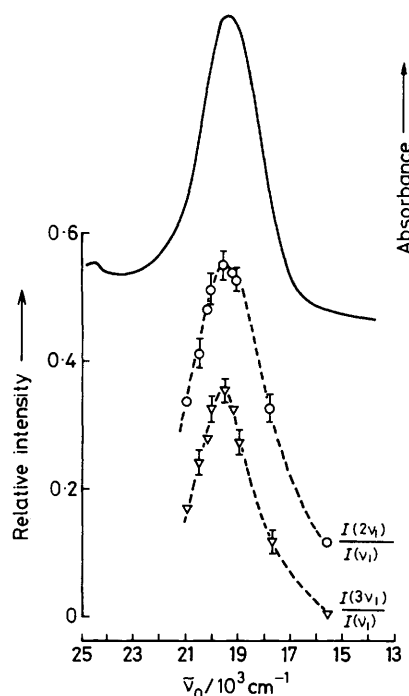


Figure 7. Plots of  $I(2\nu_1)/I(\nu_1)$  (○) and  $I(3\nu_1)/I(\nu_1)$  (▽) for  $\text{Te}_4[\text{Al}_2\text{Cl}_7]_2$ , together with the absorption spectrum of  $\text{Te}_4^{2+}$  in  $\text{H}_2\text{SO}_4$  solution

characterized by an overtone progression  $\nu_1\nu_1$  extending to  $\nu_1 = 6$  and a combination tone progression  $\nu_1\nu_1 + \nu_2$ , extending to  $\nu_1 = 3$ . No band attributable to the third Raman-active fundamental,  $\nu_3 (b_{2g})$ , is observed, apparently because its wavenumber coincides with that of  $\nu_1$  (see below). Band wavenumber measurements, assignments, bandwidths (f.w.h.m.), and depolarization ratios are given in Table 2. Excitation profiles were measured for  $\nu_1$ ,  $2\nu_1$ , and  $3\nu_1$  using the  $730 \text{ cm}^{-1}$  band of oleum as an internal standard; these are shown in Figure 5, together with the absorption spectrum of the ion.

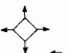

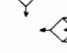
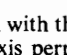
(c)  $\text{Te}_4^{2+}$ .—The lowest allowed electronic band of  $\text{Te}_4^{2+}$  (red) maximizes at 510 nm, with  $\epsilon_{\text{max.}} > 6\ 000$   $\text{dm}^3 \text{mol}^{-1} \text{cm}^{-1}$ .<sup>4</sup> Resonance Raman spectra of  $\text{Te}_4^{2+}$  in  $\text{H}_2\text{SO}_4$  solution at room temperature and of  $\text{Te}_4[\text{Al}_2\text{Cl}_7]_2$  solid at 80 K were obtained using 514.5 nm excitation. The spectrum of  $\text{Te}_4$ -

Table 3. Details of the r.R. spectrum <sup>a</sup> of Te<sub>4</sub><sup>2+</sup> in H<sub>2</sub>SO<sub>4</sub> and Te<sub>4</sub>[Al<sub>2</sub>Cl<sub>7</sub>]<sub>2</sub>


Assignment	Te <sub>4</sub> <sup>2+</sup> in H <sub>2</sub> SO <sub>4</sub> solution			Te <sub>4</sub> [Al <sub>2</sub> Cl <sub>7</sub> ] <sub>2</sub> <sup>b</sup>	
	$\tilde{\nu}/\text{cm}^{-1}$	f.w.h.m./cm <sup>-1</sup>	$\rho(\pi/2)$	$\tilde{\nu}/\text{cm}^{-1}$	f.w.h.m./cm <sup>-1</sup>
$\nu_2 (b_{1g})$	109.0 ± 0.5	8	0.75	95.0 ± 0.5	8
$\nu_1 (a_{1g})$	219.0 ± 0.5	10	0.33	213.8 ± 0.5	10
$\nu_1 (b_{2g})$					
$\nu_1 + \nu_2 (B_{1g})$				308 ± 1	15
$2\nu_1 (A_{1g})$ <sup>c</sup>	437.0 ± 0.5	15		427.0 ± 0.5	15
$3\nu_1 (A_{1g})$	655 ± 1	25		640.3 ± 0.5	24
$4\nu_1 (A_{1g})$				852.7 ± 1	40
$5\nu_1 (A_{1g})$				1 065.4 ± 1	48
$6\nu_1 (A_{1g})$				1 278 ± 2	60

<sup>a</sup>  $\lambda_0 = 514.5$  nm. <sup>b</sup> At 80 K. [Al<sub>2</sub>Cl<sub>7</sub>]<sup>-</sup> ion bands occur at 194, 342, 364, and 386 cm<sup>-1</sup>. <sup>c</sup> Possibly overlapped by  $\nu_1 + \nu_3$ .

Table 4. Wavenumbers of the fundamental modes of vibration for S<sub>4</sub><sup>2+</sup>, Se<sub>4</sub><sup>2+</sup>, and Te<sub>4</sub><sup>2+</sup>

Mode <sup>a</sup>	Form	S <sub>4</sub> <sup>2+</sup>	Se <sub>4</sub> <sup>2+</sup>	Te <sub>4</sub> <sup>2+</sup>
$\nu_1 (a_{1g})$		583.6	321.3	219
$\nu_2 (b_{1g})$		371.2	182.3	109
$\nu_3 (b_{2g})$		598.1	321.3	219
$\nu_5 (e_u)$ <sup>b</sup>		542	302	187

<sup>a</sup> *D<sub>4h</sub>* nomenclature, with the *x* and *y* axes passing through opposite atoms, and the *z* axis perpendicular to the square plane. The *v<sub>4</sub>*

(*b<sub>2u</sub>*) mode , which is analogous to the *v<sub>6</sub>* (*t<sub>2u</sub>*) mode of an MX<sub>6</sub> octahedral species, is inactive. <sup>b</sup> Ref. 15.

[Al<sub>2</sub>Cl<sub>7</sub>]<sub>2</sub>, shown in Figure 6, is characterized by an overtone progression  $\nu_1\nu_1$ , extending to  $\nu_1 = 5$ , and a combination band  $\nu_1\nu_1 + \nu_2$ . As for Se<sub>4</sub><sup>2+</sup>, the wavenumber of  $\nu_3$  (*b<sub>2g</sub>*) apparently coincides with that of  $\nu_1$ . Band wavenumber measurements, assignments, bandwidths (f.w.h.m.), and depolarization ratios are given in Table 3. It was not possible to obtain an excitation profile for Te<sub>4</sub>[Al<sub>2</sub>Cl<sub>7</sub>]<sub>2</sub>, due to the decomposition of this species when mixed with another compound as an internal intensity standard. Instead, we have plotted  $I(2\nu_1)/I(\nu_1)$  and  $I(3\nu_1)/I(\nu_1)$  for excitation within the range 476.5–647.1 nm; the results are shown in Figure 7, together with the absorption spectrum of the complex.

## Discussion

(a) *Vibrational Analysis.*—The wavenumbers of the fundamental modes of vibration of S<sub>4</sub><sup>2+</sup>, Se<sub>4</sub><sup>2+</sup>, and Te<sub>4</sub><sup>2+</sup>, including the i.r.-active  $\nu_5$  (*e<sub>u</sub>*) modes, are presented in Table 4. The band assignments for Se<sub>4</sub><sup>2+</sup> and Te<sub>4</sub><sup>2+</sup> are in agreement with those of Gillespie and co-workers<sup>6,22</sup> and therefore merit no further discussion, except for the assertion that  $\nu_3$  (*b<sub>2g</sub>*) apparently coincides with  $\nu_1$  (*a<sub>1g</sub>*) for each ion. The justification for this statement is based on two arguments.

(1) The  $\nu_3$  (*b<sub>2g</sub>*) mode is Jahn-Teller active in the <sup>1</sup>*E<sub>u</sub>* excited state (see below) and ought therefore to give rise to a band of sufficient intensity to be observed in the r.R. spectrum of each ion.

(2) The  $\rho(\pi/2)$  value measured for the band assigned to  $\nu_1$  (*a<sub>1g</sub>*) is 0.33 for both Se<sub>4</sub><sup>2+</sup> and Te<sub>4</sub><sup>2+</sup>, whereas at resonance with a  $\pi^* \leftarrow \pi$  transition, it should have the value 0.125 (see below). The  $\nu_3$  band must be depolarized, *i.e.*  $\rho(\pi/2) = 0.75$ , and the unexpected  $\rho$  value for  $\nu_1$  is due to  $\nu_1/\nu_3$  band overlap. From the measured depolarization ratio of the  $\nu_1/\nu_3$  band and those expected for  $\nu_1$  and  $\nu_3$  alone, we calculated that an

intensity ratio  $I(\nu_1)/I(\nu_3) = 1.3$  would lead to the observed  $\rho(\pi/2)$  value.

In the case of S<sub>4</sub><sup>2+</sup>, bands attributable to all three fundamentals are observed,  $\nu_3$  appearing as a shoulder 14.5 cm<sup>-1</sup> above  $\nu_1$ . Although the wavenumber of  $\nu_1$  is in agreement with the value obtained by Gillespie *et al.*<sup>9</sup> (584 cm<sup>-1</sup>), those obtained for  $\nu_2$  and  $\nu_3$  are not; the earlier values<sup>12</sup> of  $\nu_2$  (330 cm<sup>-1</sup>) and  $\nu_3$  (530 cm<sup>-1</sup>) probably arose from confusion of S<sub>4</sub><sup>2+</sup> and counter-ion bands. Our results agree closely with recently revised values of Burns and Gillespie.<sup>15</sup>

Using the wavenumber data in Table 4 we have performed a force constant calculation, employing a valence force field (VFF). The symmetry co-ordinates and *F* and *G* matrix elements for a square-planar X<sub>4</sub> type molecule have been determined by Cyvin;<sup>23</sup> these are summarized, for the in-plane vibrations, in Table 5. A generalized valence force field treatment requires eight force constants to describe the in-plane motion, but we have only four band wavenumbers; hence it is necessary to assume zero values for four of the force constants. As a first approximation we put  $f_{rr} = f_{\theta\theta} = f_{r\theta} = f_{\theta r} = 0$  and retained  $f_r, f_{rr}, f_{\theta}$ , and  $f_{\theta\theta}$ . However, the calculation produced negative values for all of the  $f_{\theta}$  and  $f_{\theta\theta}$  force constants and, furthermore, produced  $f_{\theta\theta}$  values that were of the same order as those for  $f_{\theta}$ , whereas it would normally be expected that  $f_{\theta\theta} < f_{\theta}$ . This prompted us to test a second approximation, in which  $f_{\theta\theta} = f_{\theta\theta} = f_{r\theta} = f_{\theta r} = 0$  and  $f_r, f_{rr}, f_{rr}$ , and  $f_{\theta}$  are retained. The results of this calculation are shown in Table 6. The VFF stretching force constant,  $f_r$ , decreases with increasing atomic number, *i.e.* in the order S<sub>4</sub><sup>2+</sup> (2.78 mdyne Å<sup>-1</sup>) > Se<sub>4</sub><sup>2+</sup> (2.10) > Te<sub>4</sub><sup>2+</sup> (1.45). The  $f_r$  value for S<sub>4</sub><sup>2+</sup>, with its formal (valence bond) bond order of 1.25, is almost identical with that for S<sub>3</sub><sup>-</sup> (2.77 mdyne Å<sup>-1</sup>)<sup>24</sup> which also has a formal bond order of 1.25, is less than that for S<sub>2</sub><sup>-</sup> (3.33 mdyne Å<sup>-1</sup>)<sup>24</sup> which has a formal bond order of 1.5, and is greater than that for the single-bonded species S<sub>6</sub> (2.23 mdyne Å<sup>-1</sup>),<sup>25</sup> S<sub>2</sub><sup>-</sup> (2.11),<sup>24</sup> and S<sub>3</sub><sup>2-</sup> (2.00).<sup>24</sup> Thus the  $f_r$  value for S<sub>4</sub><sup>2+</sup> fits naturally into the expected relationship between stretching force constant and bond order.

It is interesting to note that, for each ion, the interaction force constant associated with adjacent bonds,  $f_{rr}$ , is very much smaller than that associated with opposite bonds,  $f_{rr}$  (this is why the first approximation, in which  $f_{rr} = 0$ , produces unacceptable results). Indeed, it is because of this that the  $\nu_1$  and  $\nu_3$  band wavenumbers lie so close together; moreover,  $f_{rr}$  for S<sub>4</sub><sup>2+</sup> is negative, since  $\nu_3 > \nu_1$ . The values obtained for  $f_{\theta}$  are only approximate since these will include contributions from  $f_{\theta\theta}$  and  $f_{\theta\theta}$ , which, although small, may nevertheless be non-zero. No further information can be obtained that would enable  $f_{\theta\theta}$  and  $f_{\theta\theta}$  to be calculated. The remaining fundamental,  $\nu_4$  (*b<sub>2u</sub>*), which involves out-of-plane deformation motions only, will be independent of the eight in-

**Table 5.** Symmetry co-ordinates and  $G$  and  $F$  matrix elements for square-planar  $X_4$  type molecules

Symmetry species	Symmetry co-ordinate	$G$ Matrix element	$F$ Matrix element *
$A_{1g}$	$\frac{1}{2}(\Delta r_1 + \Delta r_2 + \Delta r_3 + \Delta r_4)$	$2\mu_x$	$f_r + 2f_{rr} + f_{rr'}$
$B_{1g}$	$\frac{r}{2}(\Delta\theta_{12} - \Delta\theta_{23} + \Delta\theta_{34} - \Delta\theta_{14})$	$8\mu_x$	$f_\theta - 2f_{\theta\theta} + f_{\theta\theta'}$
$B_{2g}$	$\frac{1}{2}(\Delta r_1 - \Delta r_2 + \Delta r_3 - \Delta r_4)$	$2\mu_x$	$f_r - 2f_{rr} + f_{rr'}$
$E_u$	$\frac{1}{\sqrt{12}}(\Delta r_1 - \Delta r_2 - \Delta r_3 + \Delta r_4) - \frac{r}{\sqrt{3}}(\Delta\theta_{14} - \Delta\theta_{23})$ and $\frac{1}{\sqrt{12}}(\Delta r_1 + \Delta r_2 - \Delta r_3 - \Delta r_4) - \frac{r}{\sqrt{3}}(\Delta\theta_{12} - \Delta\theta_{34})$	$6\mu_x$	$\frac{1}{2}(f_r - f_{rr'}) - \frac{2}{3}(f_{\theta\theta} - f_{\theta\theta'}) + \frac{2}{3}(f_\theta - f_{\theta\theta'})$

\*  $f_{rr}$  and  $f_{rr'}$  refer to a pair of adjacent and opposite bonds, respectively, and  $f_{\theta\theta}$  and  $f_{\theta\theta'}$  are similarly defined. For  $f_{r\theta}$  and  $f_{r\theta'}$ , the numbers of common atoms are two and one respectively;  $\mu_x$  is the reciprocal mass of the X atom.

**Table 6.** Force constants for  $S_4^{2+}$ ,  $Se_4^{2+}$ , and  $Te_4^{2+}$ 

	$S_4^{2+}$	$Se_4^{2+}$	$Te_4^{2+}$
$f_r/\text{mdyn } \text{\AA}^{-1}$	2.78	2.10	1.45
$f_{rr}/\text{mdyn } \text{\AA}^{-1}$	-0.04	0	0
$f_{rr'}/\text{mdyn } \text{\AA}^{-1}$	0.51	0.30	0.36
$f_\theta/\text{mdyn } \text{\AA}^{-1}$	0.33	0.19	0.11

**Table 7.** Harmonic wavenumbers and anharmonicity constants

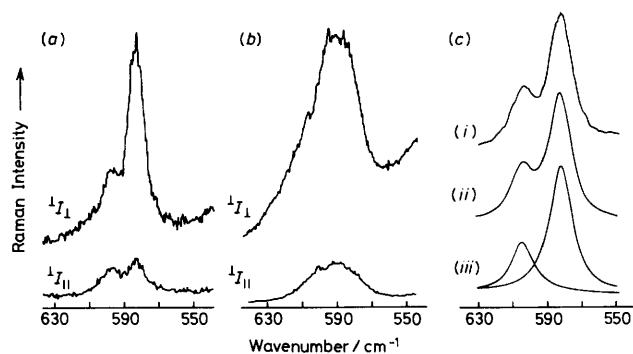
	$S_4^{2+}$	$Se_4^{2+}$	$Te_4^{2+}$	$Te_4[Al_2Cl_7]_2$
$\omega_1/\text{cm}^{-1}$	584.7	321.8	219.5	214.1
	$\pm 0.5$	$\pm 0.5$	$\pm 0.5$	$\pm 0.5$
$x_{11}/\text{cm}^{-1}$	-0.35	-0.55	-0.30	-0.16
	$\pm 0.05$	$\pm 0.05$	$\pm 0.05$	$\pm 0.05$
$x_{12}/\text{cm}^{-1}$	-0.5	-1.3		-0.8
	$\pm 1$	$\pm 1.0$		$\pm 0.5$

plane force constants. This fundamental is neither Raman nor i.r. active and has not therefore been located for the  $M_4^{2+}$  species. Its first overtone would be Raman active, but a search for this was unsuccessful. The only spectroscopic technique available for its location may be hyper-Raman spectroscopy, but as yet very few applications of this technique have been reported.<sup>26</sup>

From the wavenumber measurements of the observed overtone and combination tone progressions we have calculated a number of harmonic wavenumbers and anharmonicity constants, which are summarized in Table 7. It is noted that, in each case, the anharmonicity constant  $x_{11}$  is very small; thus the  $\nu_1$  modes in the ground state behave very nearly as harmonic oscillators, a situation which seems to prevail for most simple inorganic molecules.<sup>27</sup>

(b) *Depolarization Ratios.*—The electronic transitions of the  $M_4^{2+}$  ions around which the present r.R. studies are centred are thought<sup>20</sup> to be of the  $\pi^* \leftarrow \pi$  ( ${}^1E_u \leftarrow {}^1A_{1g}$ ) type, i.e. they are transitions which would be polarized in the  $xy$  plane. In this situation,  $\alpha_{xx} = \alpha_{yy}$  and  $\alpha_{zz} = 0$ , leading to an expected value of 0.125 for the depolarization ratios of  $a_{1g}$  modes at resonance, the  $b_{1g}$  and  $b_{2g}$  modes being depolarized. The results for  $S_4^{2+}$  are consistent with this assignment. The  $\nu_2$  ( $b_{2g}$ ) band is 14.5  $\text{cm}^{-1}$  above  $\nu_1$  ( $a_{1g}$ ) and these two bands are partially, but not totally, resolved. The measured depolarization ratios are 0.17 for  $\nu_1$  and 0.50 for  $\nu_3$ , the deviation from the expected values of 0.125 and 0.75, respectively, being ascribed to the partial overlap of the bands.

The situation for  $Se_4^{2+}$  and  $Te_4^{2+}$  is more complicated in that, for each ion, the wavenumbers of  $\nu_1$  ( $a_{1g}$ ) and  $\nu_3$  ( $b_{2g}$ ) coincide, producing a single band for which the depolarization



**Figure 8.**  $\perp I_{\perp}$  and  $\perp I_{\parallel}$  spectra of  $S_4^{2+}$  in the region 550–630  $\text{cm}^{-1}$  for spectral slitwidths of (a) 5  $\text{cm}^{-1}$  and (b) 20  $\text{cm}^{-1}$ . (c) The result of a curve analysis of the  $I_{\text{total}}$  spectrum in the region 550–630  $\text{cm}^{-1}$ : (i) experimental spectrum, (ii) calculated spectrum, (iii) resolved bands

ratio at resonance is measured to be 0.33. Although this value would be consistent with expectation for resonance with a  $z$ -polarized transition, we believe that it in fact arises from the superposition of the  $\nu_1$  and  $\nu_3$  bands, with relative intensities  $I(\nu_1)/I(\nu_3) = 1.3$ , and the expected depolarization ratios of 0.125 and 0.75. There is no polarization dispersion for the  $\nu_1/\nu_3$  bands, the depolarization ratios being the same for each ion, both on and off resonance.

Resolution of the  $\nu_1$  and  $\nu_3$  bands of  $S_4^{2+}$ , assuming Lorentzian bandshapes, enabled us to calculate the intensity ratio  $I(\nu_1)/I(\nu_3) = 2.7$ . In order to demonstrate that our calculation of  $I(\nu_1)/I(\nu_3)$  for  $Se_4^{2+}$  and  $Te_4^{2+}$  is valid, we obtained the spectrum of  $S_4^{2+}$  in the  $\nu_1/\nu_3$  region using a spectral slitwidth of 20  $\text{cm}^{-1}$ , such that a single band of symmetrical shape was observed. The measured depolarization ratio of this band is 0.24 from which it is calculated that  $I(\nu_1)/I(\nu_3) = 2.9$ , in excellent agreement with the value obtained from the resolution of the partially resolved bands in the absence of an analyser. The  $\perp I_{\perp}$  and  $\perp I_{\parallel}$  spectra for both 5  $\text{cm}^{-1}$  and 20  $\text{cm}^{-1}$  spectral slitwidths are shown in Figure 8, together with the resolution of the  $I_{\text{total}}$  spectrum. The polarization data thus confirm the assignments for the resonant electronic transitions of these ions.

(c) *Excited State Geometry.*—The observation of overtone progressions involving the totally symmetric modes in the r.R. spectra of  $S_4^{2+}$ ,  $Se_4^{2+}$ , and  $Te_4^{2+}$  is a consequence of the displacement of the excited-state potential minimum, with respect to that of the ground state, along the normal co-ordinate  $Q_1$  ( $a_{1g}$ ). That is, on excitation to the resonant state,

the M-M bond distances increase, due to transfer of an electron from an orbital which may formally be regarded as non-bonding ( $e_g$ ) to one which is antibonding ( $b_{2u}$ ).

The appearance of subsidiary progressions of the type  $v_1v_1 + v_x$  in r.R. spectra, where  $v_x$  is a non-totally symmetric fundamental, is evidence for a Jahn-Teller distortion in a degenerate excited state along the normal co-ordinate  $Q_x$ . For the  $M_d^{2+}$  species the excited state is of  ${}^1E_u$  type, the Jahn-Teller-active normal co-ordinates being  $Q_2$  ( $b_{1g}$ ) and  $Q_3$  ( $b_{2g}$ ). A progression of the type  $v_1v_1 + v_2$  is observed for all three of the ions and it is expected that  $v_1v_1 + v_3$  progressions are also present but overlapped by the  $v_1v_1$  progressions. The combination of distortions along the  $Q_2$  and  $Q_3$  co-ordinates suggests that the excited state geometry is likely to  $C_{2h}$ .

#### Acknowledgements

The authors thank the S.R.C. and the University of London for financial support, and Staveley Chemicals Ltd. for the gift of a sample of 65% oleum.

#### References

- 1 R. J. Gillespie and P. K. Ummat, *Inorg. Chem.*, 1972, **11**, 1674.
- 2 A. Bali and K. C. Malhotra, *Aust. J. Chem.*, 1975, **28**, 983.
- 3 J. Barr, R. J. Gillespie, and P. K. Ummat, *Chem. Commun.*, 1970, 264.
- 4 P. J. Stephens, *Chem. Commun.*, 1969, 1496.
- 5 R. C. Burns, R. J. Gillespie, and J. F. Sawyer, *Inorg. Chem.*, 1980, **19**, 1423.
- 6 R. J. Gillespie and G. P. Pez, *Inorg. Chem.*, 1969, **8**, 1229.
- 7 I. D. Brown, D. B. Crump, R. J. Gillespie, and D. P. Santry, *Chem. Commun.*, 1968, 853.
- 8 R. J. Gillespie and J. Passmore, *Acc. Chem. Res.*, 1971, **4**, 413.
- 9 R. J. Gillespie, J. Passmore, P. K. Ummat, and O. C. Vaidya, *Inorg. Chem.*, 1971, **10**, 1327.
- 10 I. D. Brown, D. B. Crump, and R. J. Gillespie, *Inorg. Chem.*, 1971, **10**, 2319.
- 11 R. J. Gillespie, *Chem. Soc. Rev.*, 1979, **8**, 315.
- 12 R. C. Burns, W.-L. Chan, R. J. Gillespie, W.-C. Luk, J. F. Sawyer, and D. R. Slim, *Inorg. Chem.*, 1980, **19**, 1432.
- 13 R. C. Burns, R. J. Gillespie, W.-C. Luk, and D. R. Slim, *Inorg. Chem.*, 1979, **18**, 3086.
- 14 R. C. Burns, R. J. Gillespie, J. A. Barnes, and M. J. McGlinchey, *Inorg. Chem.*, 1982, **21**, 799.
- 15 R. C. Burns and R. J. Gillespie, *Inorg. Chem.*, in the press.
- 16 T. W. Couch, D. A. Lokken, and J. D. Corbett, *Inorg. Chem.*, 1972, **11**, 357.
- 17 D. J. Prince, J. D. Corbett, and B. Garbisch, *Inorg. Chem.*, 1970, **9**, 2731.
- 18 A. Foti, V. H. Smith, and D. R. Salahub, *Chem. Phys. Lett.*, 1978, **57**, 33.
- 19 D. R. Salahub, A. E. Foti, and V. H. Smith, *J. Am. Chem. Soc.*, 1978, **100**, 7847.
- 20 K. Tanaka, T. Yamabe, H. Terama-e, and K. Fukui, *Inorg. Chem.*, 1979, **18**, 3591.
- 21 M. J. Rothman, L. S. Bartell, C. S. Ewig, and J. R. van Wazer, *J. Comput. Chem.*, 1980, **1**, 64.
- 22 M. Booth, R. J. Gillespie, and M. J. Morton, *Adv. Raman Spectrosc.*, 1973, **1**, 364.
- 23 S. J. Cyvin, 'Molecular Vibrations and Mean Square Amplitudes,' Elsevier, Amsterdam, 1968.
- 24 R. J. H. Clark and D. G. Cobbold, *Inorg. Chem.*, 1978, **17**, 3169.
- 25 L. A. Nimon and V. E. Neff, *J. Mol. Spectrosc.*, 1968, **26**, 175.
- 26 D. A. Long, *Chem. Br.*, 1971, **7**, 198.
- 27 R. J. H. Clark and B. Stewart, *Struct. Bonding (Berlin)*, 1979, **36**, 1.

Received 18th April 1982; Paper 2/469